

# UniCtrl: Improving the Spatiotemporal Consistency of Text-to-Video Diffusion Models via Training-Free Unified Attention Control

Xuweiyi Chen<sup>1,2\*</sup>, Tian Xia<sup>2\*</sup>, and Sihan Xu<sup>1,2†</sup>

<sup>1</sup> PixAI.art

<sup>2</sup> University of Michigan, Ann Arbor  
six@mewtant.io

**Abstract.** Video Diffusion Models have been developed for video generation, usually integrating text and image conditioning to enhance control over the generated content. Despite the progress, ensuring consistency across frames remains a challenge, particularly when using text prompts as control conditions. To address this problem, we introduce **UniCtrl**, a novel, plug-and-play method that is universally applicable to improve the spatiotemporal consistency and motion diversity of videos generated by text-to-video models without additional training. UniCtrl ensures semantic consistency across different frames through cross-frame self-attention control, and meanwhile, enhances the motion quality and spatiotemporal consistency through motion injection and spatiotemporal synchronization. Our experimental results demonstrate UniCtrl’s efficacy in enhancing various text-to-video models, confirming its effectiveness and universality.

**Keywords:** Video Diffusion · Spatiotemporal Consistency · Attention

## 1 Introduction

Diffusion Models (DMs) have excelled in image generation, offering enhanced stability and quality over methods like GANs [12, 26, 27] and VAEs [30, 42, 57]. Foundational studies [19, 25, 32, 48–50] established the groundwork for DMs’ capabilities in efficiently scaling up with diverse data. Recent advancements [35, 37, 41, 43, 45, 67, 69] have further improved controllability and user interaction, enabling the creation of images that better reflect user intentions.

Recently, Video Diffusion Models (VDMs) [20] have been proposed for utilizing DMs for video generation tasks. VDMs are capable of generating videos with a wide variety of motions in text-to-video synthesis tasks, supported by the integration of text encoders [40], as shown in [1, 2, 16, 18, 22, 68]. Many open-source text-to-video models have been introduced, including ModelScope [60], Animate-Diff [16], VideoCrafter [6] and so on. These models typically require a pre-trained

---

\*Authors contributed equally to this work.

†Corresponding author and project lead.



**Fig. 1:** UniCtrl for Video Generation. we propose **UniCtrl**, a concise yet effective method to significantly improve the temporal consistency of videos generated by diffusion models yet also preserve the motion. UniCtrl requires no additional training and introduces no learnable parameters, and can be treated as a plug-and-play module at inference time.

image generation model, e.g., Stable Diffusion(SD) [44], and introduce additional temporal or motion modules. However, unlike images that contain rich semantic information, text conditions are more difficult to ensure consistency between different frames of the generated video. At the same time, some work also uses image conditions to achieve image-to-video generation with improved spatial semantic consistency [1, 15, 23]. Some works have proposed the paradigm of text-to-image-to-video [11], but image conditions alone cannot effectively control the motion of videos. Combining text and image conditions leads to enhanced spatiotemporal consistency in a text-and-image-to-video workflow [6, 7, 14, 64, 70], but these methods require additional training.

To this end, our research goal in this work is to develop an effective plug-and-play method that is training-free, and can be applied to various text-to-video models to improve the performance of generated videos. To solve this problem, we first attempt to ensure that the semantic information between each frame of the video is consistent in principle. This principle draws inspiration from some previous research in attention-based control [4, 17, 56, 66]. These works have demonstrated in DMs that the queries in attention layers determine the spatial information of the generated image, and correspondingly, values determine the semantic information. We observe that this finding also holds in VDMs and propose the cross-frame self-attention control method. We thus apply the keys and values of the first frame in self-attention layers to each frame and achieve satisfying consistency in the generated video.

Secondly, we observe that as the video’s consistency improves, the motions within videos tend to become less pronounced. To solve this problem, we propose

the motion injection mechanism. Based on the assumption that queries control spatial information [4], we divide the sampling process into two branches, namely, an output branch for cross-frame self-attention control, and a motion branch without any attention control. We reserve the queries in the motion branch as motion queries, and use the corresponding motion queries in the output branch. Through the cross-frame self-attention control and motion injection, we ensure that the semantic information between each frame of the video is consistent, while the motion is preserved.

Lastly, we note that motion queries cannot guarantee the spatio-temporal consistency of video. Observing that the output of the output branch has a better spatiotemporal consistency, we further propose the spatiotemporal synchronization, that is, before each sampling step, the latent of the output branch is copied as the initial value of the latent of the motion branch. Our UniCtrl framework combines the above three methods into a plug-in-and-play method that can improve the quality of spatiotemporal consistency and motion quality of the generated videos, while ensuring the consistency of the semantic information of each frame of the video. Through experiments, several text-to-video models have been improved after applying the UniCtrl method, proving the effectiveness and universality of UniCtrl. As illustrated in Fig. 1, UniCtrl plays a significant role in improving spatiotemporal consistency and preserving motion dynamics of generated frames. This method can be readily applied during inference without the need for parameter tuning.

## 2 Related Work

**Video Generation** Many previous efforts have explored the task of video generation, e.g., GAN-based models [3, 47, 55] and transformer-based models [21, 59, 61, 62]. Recently, following that Diffusion models (DMs) [19, 25, 32, 48–50] have achieved remarkable results in image generation [36, 37, 41, 43, 45], video diffusion models (VDMs) [20] has also demonstrated their capabilities in video generation [2, 6, 7, 11, 14, 16, 18, 22, 46, 60, 64, 68]. At present, VDMs are mainly implemented by adding additional temporary layers to 2D UNet, which leads to a lack of cross-frame constraints in the training process of the 2D UNet model. Some methods [13, 39, 63] tried to use a training-free method to make the generated videos more smooth. However, how to maintain the cross-frame consistency in videos generated by VDMs remains unresolved.

**Attention Control in Diffusion Models** Different from models that require training [35, 67, 69], attention control [4, 9, 17, 56, 66] is a training-free method which has been widely applied in the task of image editing. Previous work has found that Attention Control can be used to ensure both semantic [4] and spatial consistency [9, 17, 56] in image editing. InfEdit [66] unified the control of semantic consistency and spatial consistency for the first time, proposing unified attention control (UAC). Text2Video-Zero [28] applies frame-level self-attention on text-to-image synthesis methods and enables text-to-video through manipulating motion dynamics in latent codes. Some work has introduced attention control to

VDMs for video editing [10, 29, 31], but no one has improved the consistency of generated videos through video diffusion by attention control. Is that possible to introduce UAC into VDMs to ensure cross-frame semantic consistency and spatial consistency throughout the video is an interesting and worthwhile question to explore.

### 3 Preliminary

#### 3.1 Diffusion Models (DMs)

Diffusion Models (DMs) [19, 25, 49, 50] are a type of generative model trained via score matching [24, 33, 51, 52]. The forward process gradually adds noise to data to make it follow the Gaussian distribution:  $z_t = \mathcal{N}(z_t; \sqrt{\bar{a}_t}z_0, (1 - \sqrt{\bar{a}_t})I)$ , where  $z_0$  are samples from the data distribution and  $\alpha_1, \dots, \alpha_T$  are from a variance schedule. In [19], this process is re-parameterized into the following form:

$$z_t = \sqrt{\bar{a}_t}z_0 + \sqrt{1 - \bar{a}_t}\varepsilon, \varepsilon \sim \mathcal{N}(0, I) \quad (1)$$

The training objective of DMs is predict the added noise via a neural network  $\varepsilon_\theta$ , to reconstruct the original input from the noisy sample by minimizing the distance  $d(\cdot, \cdot)$ :

$$\min_{\theta} \mathbb{E}_{z_0, \varepsilon, t} [d(\varepsilon - \varepsilon_\theta(z_t, t))] \quad (2)$$

The sampling process of DMs [19, 49] is iterative and can be represented in the form with different noise schedule  $\sigma_t$ :

$$\begin{aligned} z_{t-1} &= \sqrt{\bar{a}_{t-1}} \left( \frac{z_t - \sqrt{1 - \bar{a}_t} \varepsilon_\theta(z_t, t)}{\sqrt{\bar{a}_t}} \right) && \text{(predicted } z_0\text{)} \\ &+ \sqrt{1 - \bar{a}_{t-1} - \sigma_t^2} \cdot \varepsilon_\theta(z_t, t) && \text{(direction to } z_t\text{)} \\ &+ \sigma_t \varepsilon && \text{(random noise)} \end{aligned} \quad (3)$$

Latent Diffusion Models (LDMs) [43] encodes samples into latents using an encoder  $\mathcal{E}$ , such that  $z_0 = \mathcal{E}(x_0)$ . Also, the output is reconstructed via a decoder  $\mathcal{D}$ , represented by  $\mathcal{D}(z)$ . This approach has led to improvements in stability and efficiency in the training and generation process.

Video Diffusion Models(VDMs) [20] extended the application of DMs to the domain of video generation, adapting the framework to handle 4D video tensors in the form of  $frames \times height \times width \times channels$ , which we can use  $z_t^f$  to describe the frame  $f + 1$  at the timestep  $t$ .

#### 3.2 Attention Control

We follow the notation from [17, 66]. In the fundamental unit of the diffusion UNet model, there are two main components: cross-attention and self-attention blocks. The process begins with the linear projection of spatial features to generate queries ( $Q$ ). In the self-attention block, both keys ( $K$ ) and values ( $V$ ) are

derived from the spatial features through linear projection. Conversely, for the cross-attention part, text features undergo a linear transformation to form keys ( $K$ ) and values ( $V$ ). The attention mechanism [58] can be described as:

$$\text{ATTENTION}(Q, K, V) = \text{MV} = \text{softmax}\left(\frac{QK^T}{\sqrt{d}}\right)V \quad (4)$$

Mutual Self-Attention Control (MasaCtrl) is proposed by [4], and find that replacing the  $Q$ s in attention layers while keeping the  $K$ s and  $V$ s same, can change the spatial information of generated images but keeping the semantic information preserved. This technique can help diffusion in spatial-level editing, e.g. a sitting dog to a running dog. Here we use  $(\cdot)^{\text{src}}$  to represent the tensor obtained from the source image and  $(\cdot)^{\text{tgt}}$  for the target output we want, we can use the following formula to define the MasaCtrl algorithm.

$$out = \text{ATTENTION}(Q^{\text{tgt}}, K^{\text{src}}, V^{\text{src}})$$

Cross-Attention Control (P2P) is a method mentioned in [17], which is for semantic-level image editing (e.g. dog to cat). This work observed that different  $V$ s from different text prompts decide the semantic information of generated images. If attention maps ( $M$ ) in cross-attention layers have been reserved, but use different  $V$ s for the attention calculation, most of the spatial information will be preserved. We here use  $(\cdot)^{\text{src}}$  to represent the tensor obtained from the source image and prompt and  $(\cdot)^{\text{tgt}}$  for the target output with target prompt, this algorithm can be described as following as same  $Q^{\text{src}}, K^{\text{src}}$  lead to same  $M^{\text{src}}$ :

$$out = \text{CROSSATTENTION}(Q^{\text{src}}, K^{\text{src}}, V^{\text{tgt}})$$

## 4 UniCtrl: Cross-Frame Unified Attention Control

In the text-to-video task, it is difficult to ensure the consistency between different frames of the generated video due to the lack of semantic level conditions and the constraint of different frames in the 2D UNet layers. Based on the previous work of DMs [4, 17, 56, 66], it is found that the queries in the attention layers determine the spatial information of the generated images, and correspondingly, the values determine the semantic information. We assume these properties still exist in VDMs.

We first analyzed the role of keys and values in the self-attention layers of VDMs, and then analyzed the role of queries in all the attention layers. Inspired by InfEdit [66], we then propose the cross-frame unified attention control to achieve both semantic level consistency and better spatiotemporal consistency. Lastly, we apply spatiotemporal synchronization by replacing the latent of the motion branch with the latent from the output branch at each sampling step. We demonstrate the effectiveness of each module of UniCtrl in Fig. 2.



**Fig. 2:** The first row demonstrates the original frames generated with baseline model, which the vehicle and the road are clearly inconsistent across the frames. The second row shows frames generated with baseline model augmented with Cross-Frame Self-Attention Control (SAC). While it maintains incredible spatiotemporal consistency, it exhibits little motion. The third row explains frames augmented with SAC and Motion Injection (MI). Although MI injects more motion in addition to SAC, the results clear demonstrate that it falls short on spatiotemporal consistency again. The fourth row contains frames further augmented with Spatiotemporal Synchronization (SS) in addition to SAC and MI, which improves spatiotemporal consistency over the results from the third row and achieved balance between motion and spatiotemporal consistency, both in-frame and cross-frame.

#### 4.1 Cross-Frame Self-Attention Control

Previous work [4, 17, 56, 66] has observed that queries in the attention mechanism form the layout and semantic information of generated images [4, 56, 66], while values contribute to the semantic information [17, 66]. Therefore, we hypothesize that using the same values in the attention of different frames can ensure cross-frame consistency. Additionally, we observed that the mismatch between keys and values will degrade the quality of generated videos through our experiment and we provide one qualitative example in Section 5.4. Consequently, in our cross-frame Self-Attention Control (SAC), we inject both keys and values from the first frame, as detailed in Algorithm 1, to every other frame at each self-attention layer during denoising. We showcase one example of the effectiveness of SAC by comparing the first row and the second row in Fig. 2.

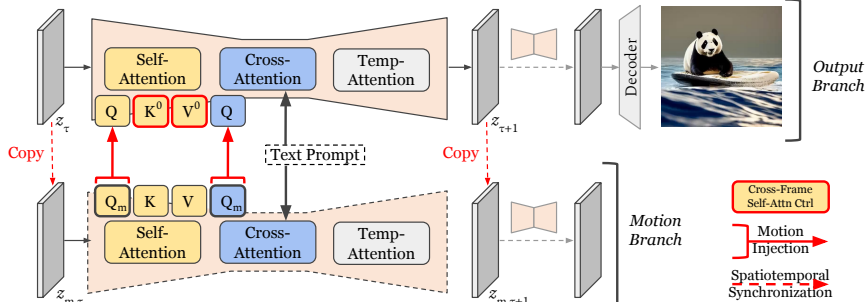


**Fig. 3:** In our framework, we use key and value from the first frame as represented by  $K^0$  and  $V^0$  in the self-attention block. We also use another branch to keep the motion query  $Q_m$  for motion control. At the beginning of every sampling step, we let the motion latent equal to the sampling latent, to avoid spatial-temporal inconsistency. We explain details of our framework in Algorithm 1 and Algorithm 2.

#### 4.2 Motion Injection

In our experiments, detailed in Section 5, we identify a significant limitation associated with cross-frame self-attention control: it tends to produce overly similar consecutive frames, leading to minimal motion within the video sequence. Again, as described in [4, 66], the queries in self-attention and cross-attention determine the video’s spatial information, which corresponds to motion. Therefore, by preserving the original queries, we can maintain the motion effect.

As in Fig. 3, we have divided the inference process into two branches: the output branch, which undergoes cross-frame self-attention control, and the motion branch, which does not involve attention control. We retain the queries in the motion branch as motion queries and use the corresponding motion queries in the output branch. Here, we denote motion queries as  $Q_m$ . The method for motion injection can be expressed by the following formula:  $out = \text{ATTENTION}(Q_m, \cdot, \cdot)$ , where ATTENTION refers to both of self- and cross-attention layers. This method is designed to fully retain the motion of the original video. However, in practice, a trade-off between motion preservation and spatiotemporal coherence remains evident. Consequently, we propose an additional refinement: selectively preserv-

---

#### Algorithm 1 Cross-Frame Self-Attention Control

---

- 1: **Input:** Hidden State  $z$
  - 2:  $bs, c, f, h, w = z.\text{shape}()$
  - 3:  $z^0 = z[:, :, 0, :, :].\text{unsqueeze}(2)$  # Extract the first frame.
  - 4:  $z^0 = z^0.\text{repeat}(1, 1, f, 1, 1)$
  - 5:  $Q = \text{to\_q}(z)$
  - 6:  $K^0 = \text{to\_k}(z^0)$  # Obtain the Key of the first frame.
  - 7:  $V^0 = \text{to\_v}(z^0)$  # Obtain the Value of the first frame,
  - 8:  $out = \text{SELFATTENTION}(Q, K^0, V^0)$
  - 9: **Output:**  $out$
-

ing motion at specific steps throughout the sampling process to enhance control. To this end, we introduce a technique that modulates motion through the integration of a motion injection degree,  $c$ , which is defined within the interval  $0 \leq c \leq 1$ . The following outlines this approach in detail:

$$out = \begin{cases} \text{ATTENTION}(Q_m, \cdot, \cdot) & t \geq (1 - c) \times T \\ \text{ATTENTION}(Q, \cdot, \cdot) & t < (1 - c) \times T \end{cases}$$

### 4.3 Spatiotemporal Synchronization

Upon closer inspection of the results, notably exemplified by the third row of Figure 2, it becomes evident that simply injecting spatial information from the original video is insufficient for guaranteeing spatiotemporal consistency. Considering that output branch yields more spatiotemporally consistent results, we further propose **Spatiotemporal Synchronization (SS)**: the latent of the output branch is copied as the initial value of the latent for the motion branch before each sampling step. By doing so, our method can simultaneously ensure the semantic consistency of the generated video and improve the quality of spatiotemporal consistency and preserve the degree of motion diversity. We present a qualitative example to demonstrate the effectiveness of SS by comparing the results depicted in the third and fourth rows of Figure 2.

---

#### Algorithm 2 Cross-Frame Unified Attention Control

---

```

1: Input:
    Video Diffusion Model VDM
    Sequence of timesteps  $\tau_0 > \tau_1 > \dots > \tau_N$ 
    Text Condition  $c$ 
    Controlled Self Attention Algorithm SELFATTNCTRL
    Timestep condition for Motion Control  $t$ 
2:  $z_{m,\tau_0} = z_{\tau_0} \sim \mathcal{N}(\mathbf{0}, \mathbf{I})$ 
3: VDM.SELFATTN = SELFATTNCTRL
4: for  $n = 0$  to  $N - 1$  do
5:    $z_{m,\tau_n} = z_{\tau_n}$ 
6:    $Q_m \leftarrow \mathbf{VDM}(z_{m,\tau_n}, c, \tau_n)$ 
7:   if  $t \geq \tau_n$  then
8:      $z_{\tau_{n+1}} = \mathbf{VDM}(z_{\tau_n}, c, \tau_n)\{Q \leftarrow Q_m\}$ 
9:   else
10:     $z_{\tau_{n+1}} = \mathbf{VDM}(z_{\tau_n}, c, \tau_n)$ 
11:   end if
12: end for
13: Output:  $z_{\tau_N}$ 

```

---

### 4.4 Cross-Frame Unified Attention Control

As illustrated in Figure 3, we integrate Cross-Frame Self-Attention Control, Motion Injection and Spatiotemporal Synchronization into a cohesive framework termed Cross-Frame Unified Attention Control. In the output branch, we

employ the key  $K^0$  and value  $V^0$  derived from the initial frame to maintain cross-frame semantic consistency. A separate branch is utilized to preserve the query specifically for motion control, replacing the output branch’s query with  $Q_m$  from the motion control branch. To prevent spatiotemporal inconsistencies, we synchronize the latent representation of the motion branch with the output branch’s preceding latent state before each sampling step. This approach is further detailed presented in Algorithm 2.

## 5 Experiments

In this section, we evaluate the effectiveness of UniCtrl. We discuss metrics, backbones and baseline in Section 5.1. Then we include both qualitative comparisons in Section 5.2 and quantitative comparisons in Section 5.3 to showcase the effectiveness of UniCtrl in terms spatiotemporal consistency and motion preservation. Additionally, we explore the contribution of each component within UniCtrl, the motion injection degree, and the specific design choice of swapping Key and Value together in the SAC procedure, as detailed in Section 5.4.

### 5.1 Experimental Setup

To evaluate the effectiveness of our model, we collect prompts from two datasets UCF-101 [53] and MSR-VTT [65] for generating videos. Following Ge et al [8], we use the same UCF-101 prompts for our experiments. We also randomly select 100 unique prompts from the MSR-VTT dataset for our evaluation. Those two parts of data consist of our dataset for evaluations. Next we briefly introduce evaluation metrics and we will provide details in the supplementary material.

**Metric** To quantitatively evaluate our results, we consider standard metrics following [46, 63]:

- *DINO*: To evaluate the spatiotemporal consistency in the generated video, we employ DINO [38] to compare the cosine similarity between initial frame and subsequent frames. In our experiments, we utilize the DINO-vits16 [5] model to compute the DINO cosine similarity.
- *RAFT*: To compare the magnitude of motion in the videos, we utilize RAFT [54] to estimate the optical flow, thereby inferring the degree of motion. We utilize the off-the-shelf RAFT model from torchvision [34].

**Backbones** Since our method is plug-and-play, we decide to evaluate our methods on a few popular baselines:

- *AnimateDiff* [16] introduces a practical framework for adding motion dynamics to personalized text-to-image models, such as those created by Stable Diffusion, without the need for model-specific adjustments. Central to AnimateDiff is a motion module, trainable once and universally applicable across personalized text-to-image models derived from the same base model, leveraging transferable motion priors from real-world videos for animation.

**Table 1:** Quantitative Comparisons on UCF-101 and MSR-VTT. UniCtrl significantly improves the temporal consistency while keeps the motion in the generated videos.  $c$  indicates the motion injection degree.  $I$  indicates number of iteration for FreeInit.

Method	DINO ( $\uparrow$ )	RAFT ( $\uparrow$ )
AnimateDiff [16]	93.99	31.38
FreeInit + AnimateDiff ( $I = 3$ )	96.15	14.79
UniCtrl + AnimateDiff ( $c = 1$ )	96.34 <sub>(+00.19)</sub>	25.70 <sub>(+10.91)</sub>
VideoCrafter [6]	93.39	28.25
FreeInit + VideoCrafter ( $I = 3$ )	96.61	6.90
UniCtrl + VideoCrafter ( $c = 1$ )	94.13 <sub>(-02.48)</sub>	28.78 <sub>(+21.88)</sub>
UniCtrl + FreeInit + AnimateDiff ( $I = 3, c = 1$ )	96.48	17.91

- *VideoCrafter* [6] introduces two novel diffusion models for video generation: T2V, which synthesizes high-quality videos from text inputs, achieving cinematic-quality resolutions up to  $1024 \times 576$ , and I2V, the first open-source model that transforms images into videos while preserving content, structure, and style. Both models represent significant advancements in open-source video generation technology, offering new tools for researchers and engineers. We use T2V version in our experiments.

**Baseline** We select FreeInit [63] as our baseline since FreeInit is a training free method that attempts to improve subject appearance and temporal consistency of generated videos through iteratively refining the spatial-temporal low-frequency components of the initial latent during inference. However, given that our method UniCtrl operates on the attention mechanism and FreeInit adjusts the frequency domain of the latent space, UniCtrl and FreeInit are orthogonal approaches. Both are training-free methods capable of enhancing the spatiotemporal consistency of generated videos via diffusion models. We demonstrate the integration of UniCtrl and FreeInit both in 5.2 and 5.3.

## 5.2 Quatitative Comparisons

Qualitative comparisons, depicted in Figure 4, reveal that our UniCtrl method markedly improves spatiotemporal consistency and maintains motion diversity. For example, with the text prompt "walking with a dog", FreeInit produces inconsistent appearances for both the lady and the dog, whereas UniCtrl ensures consistent representations of both entities. Furthermore, when processing the prompt "A young woman walks through flashing lights", UniCtrl maintains the detailed features of the young woman's dress while ensuring her walking motion remains natural, in contrast to the vanilla AnimateDiff model. Additionally, we demonstrate UniCtrl's flawless integration with FreeInit, enhancing motion in the background while consistently preserving the young woman's appearance. Additional qualitative findings can be found in the supplementary material.

## 5.3 Quanlitative Comparisons

For quantitative comparisons, the quantitative results on UCF-101 and MSR-VTT are reported in Table 1. We compare the backbones and backbones aug-



**Fig. 4: Qualitative Comparisons.** We showcase UniCtrl’s adaptability to varied text prompts, leveraging UniCtrl to significantly improve temporal consistency and preserve motion diversity. Comparative inference results with FreeInit are presented for context. Additionally, we demonstrate UniCtrl’s seamless integration with FreeInit.

**Table 2:** Ablation results on UCF-101 and MSR-VTT. We ablate each module of UniCtrl and show the effectiveness of them each.  $c$  indicates the motion injection degree.

Method	DINO ( $\uparrow$ )	RAFT
AnimateDiff [16]	93.99	31.81
UniCtrl w/o SAC + AnimateDiff	93.99	31.81
UniCtrl w/o MI + AnimateDiff	97.98	4.19
UniCtrl w/o SS + AnimateDiff	93.98	31.78
UniCtrl ( $c = 0$ ) + AnimateDiff	97.98	4.19
UniCtrl ( $c = 0.2$ ) + AnimateDiff	97.36	9.73
UniCtrl ( $c = 0.4$ ) + AnimateDiff	96.62	16.15
UniCtrl ( $c = 0.6$ ) + AnimateDiff	96.41	22.14
UniCtrl ( $c = 0.8$ ) + AnimateDiff	96.34	24.60
UniCtrl ( $c = 1.0$ ) + AnimateDiff	96.34	25.70

mented by UniCtrl and FreeInit respectively. According to the metrics, UniCtrl significantly improves the spatiotemporal consistency in the generated videos across all backbones on both prompt sets from 0.74 to 2.35. While FreeInit achieves remarkable improvements over spatiotemporal consistency, we found that UniCtrl outperforms FreeInit on the strength of motions on both AnimateDiff and VideoCrafter by a large margin from 10.91 to 21.88. Note that we purposely choose the motion injection degree  $c = 1$  to demonstrate how UniCtrl can preserve the motion compare with FreeInit. However, there still exists a trade off between spatiotemporal consistency and motion diversity. In section 5.4, we show spatiotemporal consistency can be further improved with a smaller motion injection degree. Thus, we recommend motion injection degree  $c = 0.4$  for real-world applications. Lastly, we showcase how UniCtrl and FreeInit can improve AnimateDiff together and we found this integration can improve both spatiotemporal consistency and motion diversity. We will introduce the details how we integrate UniCtrl and FreeInit in the supplementary material. Note that we obtained different score for FreeInit because we randomly sampled a different set of prompts from MSR-VTT and we used our own implementations for FreeInit on VideoCrafter since we cannot find official implementation.

#### 5.4 Ablation Study

We assess the impact of each UniCtrl module, the efficacy of motion injection degree, and corroborate our design choice of swapping Key and Value together in the SAC procedure through the subsequent ablation studies.

**Evaluating the Impact of SAC, MI, and SS** To assess the contribution of the SAC, we conducted experiments on both datasets using AnimateDiff as the baseline, incorporating our pipeline but disabling SAC. For motion injection, we set motion injection degree to be 1. The findings reveal our method without SAC works exactly the same the backbone because the motion branch is the exactly the same as the output branch. This observation underscores the critical role of SAC in enhancing spatiotemporal consistency, as evidenced by the comparisons with the scores fom the vanilla AnimateDiff.

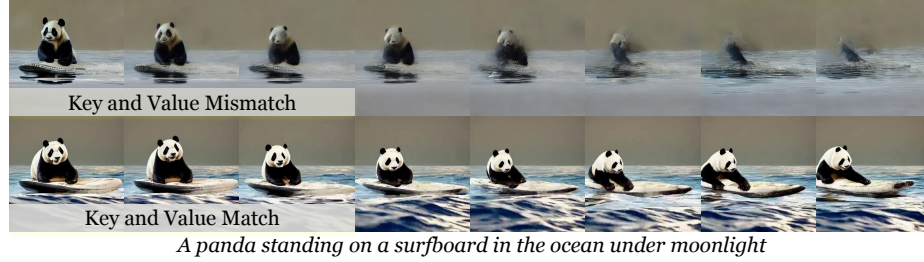


**Fig. 5:** Each row displays a sequence of video frames generated from the identical prompt: A panda standing on a surfboard in the ocean under moonlight. The section labeled **K and V mismatch** illustrates the frames produced when there is a discrepancy between key and value pairs. Conversely, the section titled **K and V match** showcases frames generated when key and value pairs are in alignment.

In exploring the significance of Motion Injection (MI), additional tests were performed on both datasets with AnimateDiff serving as the baseline, this time with MI deactivated. The results indicated a notable consistency with the baseline, yet with a substantial reduction in motion diversity. This was quantitatively supported by a decrease in the RAFT score from 31.81 to 4.19. Such a marked disparity highlights MI’s vital contribution to maintaining the motion dynamics.

Finally, the necessity of the Stabilization Strategy (SS) was examined by excluding SS from our pipeline and conducting experiments across both datasets, again using AnimateDiff as the reference point and setting motion injection degree to be 1. The outcomes showed diminished spatiotemporal consistency in comparison to the baseline, while motion diversity was not significantly impacted. These results emphasize the importance of integrating SS into our pipeline, as corroborated by the UniCtrl’s findings presented in Table 1, illustrating the essential role of SS in achieving the desired balance of spatiotemporal consistency and motion diversity.

**Influence of Motion Injection Degree** To assess the impact of varying degrees of motion injection, we conducted experiments across both datasets using UniCtrl with motion injection degree set at  $c = 0$ ,  $c = 0.2$ ,  $c = 0.4$ ,  $c = 0.6$ ,  $c = 0.8$ , and  $c = 1$ . The effects of different motion injection levels are depicted quantitatively in Table 2. As the degree of motion injection escalates, we observed that the DINO score consistently outperforms baseline metrics, and the RAFT score progressively increases. This trend indicates an amplification in motion diversity. We showcase qualitative examples of the influence of motion injection degree in the supplementary material.

**Influence of Swapping Key and Value** We aim to provide a qualitative example to underscore the importance of simultaneously modifying both key and value, as highlighted in our discussion on the impact of key and value mismatches in Section 4.1. Initially, we alter only the value while maintaining the same key within the Spatial Attention Component (SAC) performing the UniCtrl pipeline. As depicted in the first row of Fig. 5, the panda begins to fade in the subsequent frames, indicating a substantial decrease in the quality of the

generated videos with respect to spatiotemporal consistency. This decline is particularly evident when compared to the approach of modifying both the key and value concurrently using the same UniCtrl pipeline.

## 6 Conclusion

We introduce UniCtrl to address the challenges of maintaining cross-frame consistency and preserving motions for Video Diffusion Models. By incorporating UniCtrl, we have notably improved the spatiotemporal consistency across frames of generated videos. Our approach stands out as it requires no additional training, making it adaptable to various underlying models. The efficacy of UniCtrl has been rigorously tested, demonstrating its potential to be widely applied to text-to-video generative models. We discuss the primary limitations of UniCtrl in Section 6.1 and detail our ethics statement in Section 6.2.

### 6.1 Limitations

Our method needs to operate on the attention mechanism, which limits the application of our method on non-attention-based models. Also, since we ensure the same value for each frame, changing colors within the video is not possible, which limits the model’s ability to generate videos. Additionally, we have not yet guaranteed that spatial information is completely consistent across frames; this might be addressed in future work by controlling the temporal attention block. Furthermore, during the inference process, we need additional computation to preserve the motion query, which affects the inference speed. Our method can still be improved by addressing the above issues.

### 6.2 Ethics Statement

While UniCtrl offers significant advancements in video generation, it is imperative to consider its broader ethical, legal, and societal implications.

**Copyright Infringement.** As an advanced video generation tool, UniCtrl could be utilized to modify and repurpose original video works, raising concerns over copyright infringement. It is crucial for users to respect the rights of content creators and uphold the integrity of the creative industry by adhering to copyright and licensing laws.

**Deceptive Misuse.** Given its ability to generate high-quality, consistent video content, there is a risk that UniCtrl could be exploited for deceptive purposes, such as creating misleading or fraudulent content. This underscores the need for responsible usage guidelines and robust security measures to prevent such malicious applications and protect against security threats.

**Bias and Fairness.** UniCtrl relies on underlying diffusion models that may harbor inherent biases, potentially leading to fairness issues in the generated content. Although our method is algorithmic and not directly trained on large-scale datasets, it is essential to acknowledge and address any biases present in these foundational models to ensure equitable and ethical utilization.

By proactively addressing these ethical considerations, we can responsibly leverage the capabilities of UniCtrl, ensuring its application aligns with legal standards and societal welfare. Emphasizing ethical practices, legal compliance, and the well-being of society is paramount in advancing video generation technology while maintaining public trust and upholding community values.

## References

1. Blattmann, A., Dockhorn, T., Kulal, S., Mendelevitch, D., Kilian, M., Lorenz, D., Levi, Y., English, Z., Voleti, V., Letts, A., et al.: Stable video diffusion: Scaling latent video diffusion models to large datasets. arXiv preprint arXiv:2311.15127 (2023)
2. Blattmann, A., Rombach, R., Ling, H., Dockhorn, T., Kim, S.W., Fidler, S., Kreis, K.: Align your latents: High-resolution video synthesis with latent diffusion models. In: Proceedings of the IEEE/CVF Conference on Computer Vision and Pattern Recognition. pp. 22563–22575 (2023)
3. Brooks, T., Hellsten, J., Aittala, M., Wang, T.C., Aila, T., Lehtinen, J., Liu, M.Y., Efros, A., Karras, T.: Generating long videos of dynamic scenes. Advances in Neural Information Processing Systems **35**, 31769–31781 (2022)
4. Cao, M., Wang, X., Qi, Z., Shan, Y., Qie, X., Zheng, Y.: Masactrl: Tuning-free mutual self-attention control for consistent image synthesis and editing. In: Proceedings of the IEEE/CVF International Conference on Computer Vision (ICCV). pp. 22560–22570 (October 2023)
5. Caron, M., Touvron, H., Misra, I., Jégou, H., Mairal, J., Bojanowski, P., Joulin, A.: Emerging properties in self-supervised vision transformers (2021)
6. Chen, H., Xia, M., He, Y., Zhang, Y., Cun, X., Yang, S., Xing, J., Liu, Y., Chen, Q., Wang, X., Weng, C., Shan, Y.: Videocrafter1: Open diffusion models for high-quality video generation (2023)
7. Chen, H., Zhang, Y., Cun, X., Xia, M., Wang, X., Weng, C., Shan, Y.: Videocrafter2: Overcoming data limitations for high-quality video diffusion models (2024)
8. Ge, S., Nah, S., Liu, G., Poon, T., Tao, A., Catanzaro, B., Jacobs, D., Huang, J.B., Liu, M.Y., Balaji, Y.: Preserve your own correlation: A noise prior for video diffusion models (2023)
9. Ge, S., Park, T., Zhu, J.Y., Huang, J.B.: Expressive text-to-image generation with rich text. In: IEEE International Conference on Computer Vision (ICCV) (2023)
10. Geyer, M., Bar-Tal, O., Bagon, S., Dekel, T.: Tokenflow: Consistent diffusion features for consistent video editing. arXiv preprint arXiv:2307.10373 (2023)
11. Girdhar, R., Singh, M., Brown, A., Duval, Q., Azadi, S., Rambhatla, S.S., Shah, A., Yin, X., Parikh, D., Misra, I.: Emu video: Factorizing text-to-video generation by explicit image conditioning. arXiv preprint arXiv:2311.10709 (2023)
12. Goodfellow, I., Pouget-Abadie, J., Mirza, M., Xu, B., Warde-Farley, D., Ozair, S., Courville, A., Bengio, Y.: Generative adversarial networks. Communications of the ACM **63**(11), 139–144 (2020)
13. Gu, J., Wang, S., Zhao, H., Lu, T., Zhang, X., Wu, Z., Xu, S., Zhang, W., Jiang, Y.G., Xu, H.: Reuse and diffuse: Iterative denoising for text-to-video generation. arXiv preprint arXiv:2309.03549 (2023)
14. Gu, X., Wen, C., Song, J., Gao, Y.: Seer: Language instructed video prediction with latent diffusion models. arXiv preprint arXiv:2303.14897 (2023)

15. Guo, Y., Yang, C., Rao, A., Agrawala, M., Lin, D., Dai, B.: Sparsectrl: Adding sparse controls to text-to-video diffusion models. arXiv preprint arXiv:2311.16933 (2023)
16. Guo, Y., Yang, C., Rao, A., Wang, Y., Qiao, Y., Lin, D., Dai, B.: Animatediff: Animate your personalized text-to-image diffusion models without specific tuning. arXiv preprint arXiv:2307.04725 (2023)
17. Hertz, A., Mokady, R., Tenenbaum, J., Aberman, K., Pritch, Y., Cohen-or, D.: Prompt-to-prompt image editing with cross-attention control. In: The Eleventh International Conference on Learning Representations (2023), [https://openreview.net/forum?id=\\_CDixzkzeyb](https://openreview.net/forum?id=_CDixzkzeyb)
18. Ho, J., Chan, W., Saharia, C., Whang, J., Gao, R., Gritsenko, A., Kingma, D.P., Poole, B., Norouzi, M., Fleet, D.J., et al.: Imagen video: High definition video generation with diffusion models. arXiv preprint arXiv:2210.02303 (2022)
19. Ho, J., Jain, A., Abbeel, P.: Denoising diffusion probabilistic models. Advances in neural information processing systems **33**, 6840–6851 (2020)
20. Ho, J., Salimans, T., Gritsenko, A., Chan, W., Norouzi, M., Fleet, D.J.: Video diffusion models. Advances in Neural Information Processing Systems (2022)
21. Hong, W., Ding, M., Zheng, W., Liu, X., Tang, J.: Cogvideo: Large-scale pretraining for text-to-video generation via transformers. arXiv preprint arXiv:2205.15868 (2022)
22. Hu, Y., Luo, C., Chen, Z.: Make it move: controllable image-to-video generation with text descriptions. In: Proceedings of the IEEE/CVF Conference on Computer Vision and Pattern Recognition. pp. 18219–18228 (2022)
23. Hu, Z., Xu, D.: Videocontrolnet: A motion-guided video-to-video translation framework by using diffusion model with controlnet. arXiv preprint arXiv:2307.14073 (2023)
24. Hyvärinen, A., Dayan, P.: Estimation of non-normalized statistical models by score matching. Journal of Machine Learning Research **6**(4) (2005)
25. Karras, T., Aittala, M., Aila, T., Laine, S.: Elucidating the design space of diffusion-based generative models. Advances in Neural Information Processing Systems **35**, 26565–26577 (2022)
26. Karras, T., Laine, S., Aila, T.: A style-based generator architecture for generative adversarial networks. In: Proceedings of the IEEE/CVF conference on computer vision and pattern recognition. pp. 4401–4410 (2019)
27. Karras, T., Laine, S., Aittala, M., Hellsten, J., Lehtinen, J., Aila, T.: Analyzing and improving the image quality of StyleGAN. In: Proc. CVPR (2020)
28. Khachatryan, L., Movsisyan, A., Tadevosyan, V., Henschel, R., Wang, Z., Navasardyan, S., Shi, H.: Text2video-zero: Text-to-image diffusion models are zero-shot video generators. arXiv preprint arXiv:2303.13439 (2023)
29. Khandelwal, A.: Infusion: Inject and attention fusion for multi concept zero-shot text-based video editing. In: Proceedings of the IEEE/CVF International Conference on Computer Vision. pp. 3017–3026 (2023)
30. Kingma, D.P., Welling, M.: Auto-encoding variational bayes. In: International Conference on Learning Representations (2014)
31. Liu, S., Zhang, Y., Li, W., Lin, Z., Jia, J.: Video-p2p: Video editing with cross-attention control. arXiv preprint arXiv:2303.04761 (2023)
32. Luo, S., Tan, Y., Huang, L., Li, J., Zhao, H.: Latent consistency models: Synthesizing high-resolution images with few-step inference. arXiv preprint arXiv:2310.04378 (2023)
33. Lyu, S.: Interpretation and generalization of score matching. arXiv preprint arXiv:1205.2629 (2012)

34. maintainers, T., contributors: Torchvision: Pytorch's computer vision library. <https://github.com/pytorch/vision> (2016)
35. Mou, C., Wang, X., Xie, L., Zhang, J., Qi, Z., Shan, Y., Qie, X.: T2i-adapter: Learning adapters to dig out more controllable ability for text-to-image diffusion models. arXiv preprint arXiv:2302.08453 (2023)
36. Nichol, A.Q., Dhariwal, P.: Improved denoising diffusion probabilistic models. In: International Conference on Machine Learning. pp. 8162–8171. PMLR (2021)
37. Nichol, A.Q., Dhariwal, P., Ramesh, A., Shyam, P., Mishkin, P., McGrew, B., Sutskever, I., Chen, M.: Glide: Towards photorealistic image generation and editing with text-guided diffusion models. In: International Conference on Machine Learning. pp. 16784–16804. PMLR (2022)
38. Oquab, M., Darcet, T., Moutakanni, T., Vo, H., Szafraniec, M., Khalidov, V., Fernandez, P., Haziza, D., Massa, F., El-Nouby, A., Assran, M., Ballas, N., Galuba, W., Howes, R., Huang, P.Y., Li, S.W., Misra, I., Rabbat, M., Sharma, V., Synnaeve, G., Xu, H., Jegou, H., Mairal, J., Labatut, P., Joulin, A., Bojanowski, P.: Dinov2: Learning robust visual features without supervision (2024)
39. Qiu, H., Xia, M., Zhang, Y., He, Y., Wang, X., Shan, Y., Liu, Z.: Freenoise: Tuning-free longer video diffusion via noise rescheduling. arXiv preprint arXiv:2310.15169 (2023)
40. Radford, A., Kim, J.W., Hallacy, C., Ramesh, A., Goh, G., Agarwal, S., Sastry, G., Askell, A., Mishkin, P., Clark, J., et al.: Learning transferable visual models from natural language supervision. In: International conference on machine learning. pp. 8748–8763. PMLR (2021)
41. Ramesh, A., Dhariwal, P., Nichol, A., Chu, C., Chen, M.: Hierarchical text-conditional image generation with clip latents. arXiv preprint arXiv:2204.06125 **1**(2), 3 (2022)
42. Ramesh, A., Pavlov, M., Goh, G., Gray, S., Voss, C., Radford, A., Chen, M., Sutskever, I.: Zero-shot text-to-image generation. In: International Conference on Machine Learning. pp. 8821–8831. PMLR (2021)
43. Rombach, R., Blattmann, A., Lorenz, D., Esser, P., Ommer, B.: High-resolution image synthesis with latent diffusion models. In: Proceedings of the IEEE/CVF conference on computer vision and pattern recognition. pp. 10684–10695 (2022)
44. Rombach, R., Blattmann, A., Lorenz, D., Esser, P., Ommer, B.: High-resolution image synthesis with latent diffusion models (2022)
45. Saharia, C., Chan, W., Saxena, S., Li, L., Whang, J., Denton, E.L., Ghasemipour, K., Gontijo Lopes, R., Karagol Ayan, B., Salimans, T., et al.: Photorealistic text-to-image diffusion models with deep language understanding. Advances in Neural Information Processing Systems **35**, 36479–36494 (2022)
46. Singer, U., Polyak, A., Hayes, T., Yin, X., An, J., Zhang, S., Hu, Q., Yang, H., Ashual, O., Gafni, O., et al.: Make-a-video: Text-to-video generation without text-video data. arXiv preprint arXiv:2209.14792 (2022)
47. Skorokhodov, I., Tulyakov, S., Elhoseiny, M.: Stylegan-v: A continuous video generator with the price, image quality and perks of stylegan2. In: Proceedings of the IEEE/CVF Conference on Computer Vision and Pattern Recognition. pp. 3626–3636 (2022)
48. Sohl-Dickstein, J., Weiss, E., Maheswaranathan, N., Ganguli, S.: Deep unsupervised learning using nonequilibrium thermodynamics. In: International conference on machine learning. pp. 2256–2265. PMLR (2015)
49. Song, J., Meng, C., Ermon, S.: Denoising diffusion implicit models. In: International Conference on Learning Representations (2020)

50. Song, Y., Dhariwal, P., Chen, M., Sutskever, I.: Consistency models. arXiv preprint arXiv:2303.01469 (2023)
51. Song, Y., Ermon, S.: Generative modeling by estimating gradients of the data distribution. Advances in neural information processing systems **32** (2019)
52. Song, Y., Sohl-Dickstein, J., Kingma, D.P., Kumar, A., Ermon, S., Poole, B.: Score-based generative modeling through stochastic differential equations. arXiv preprint arXiv:2011.13456 (2020)
53. Soomro, K., Zamir, A.R., Shah, M.: Ucf101: A dataset of 101 human actions classes from videos in the wild (2012)
54. Teed, Z., Deng, J.: Raft: Recurrent all-pairs field transforms for optical flow (2020)
55. Tian, Y., Ren, J., Chai, M., Olszewski, K., Peng, X., Metaxas, D.N., Tulyakov, S.: A good image generator is what you need for high-resolution video synthesis. arXiv preprint arXiv:2104.15069 (2021)
56. Tumanyan, N., Geyer, M., Bagon, S., Dekel, T.: Plug-and-play diffusion features for text-driven image-to-image translation. In: Proceedings of the IEEE/CVF Conference on Computer Vision and Pattern Recognition (CVPR). pp. 1921–1930 (June 2023)
57. Van Den Oord, A., Vinyals, O., et al.: Neural discrete representation learning. Advances in neural information processing systems **30** (2017)
58. Vaswani, A., Shazeer, N., Parmar, N., Uszkoreit, J., Jones, L., Gomez, A.N., Kaiser, Ł., Polosukhin, I.: Attention is all you need. Advances in neural information processing systems **30** (2017)
59. Villegas, R., Babaeizadeh, M., Kindermans, P.J., Moraldo, H., Zhang, H., Saffar, M.T., Castro, S., Kunze, J., Erhan, D.: Phenaki: Variable length video generation from open domain textual description. arXiv preprint arXiv:2210.02399 (2022)
60. Wang, J., Yuan, H., Chen, D., Zhang, Y., Wang, X., Zhang, S.: Modelscope text-to-video technical report (2023)
61. Wu, C., Huang, L., Zhang, Q., Li, B., Ji, L., Yang, F., Sapiro, G., Duan, N.: Godiva: Generating open-domain videos from natural descriptions. arXiv preprint arXiv:2104.14806 (2021)
62. Wu, C., Liang, J., Ji, L., Yang, F., Fang, Y., Jiang, D., Duan, N.: Nüwa: Visual synthesis pre-training for neural visual world creation. In: European conference on computer vision. pp. 720–736. Springer (2022)
63. Wu, T., Si, C., Jiang, Y., Huang, Z., Liu, Z.: Freeinit: Bridging initialization gap in video diffusion models. arXiv preprint arXiv:2312.07537 (2023)
64. Xing, J., Xia, M., Zhang, Y., Chen, H., Wang, X., Wong, T.T., Shan, Y.: Dynamicrofter: Animating open-domain images with video diffusion priors. arXiv preprint arXiv:2310.12190 (2023)
65. Xu, J., Mei, T., Yao, T., Rui, Y.: Msr-vtt: A large video description dataset for bridging video and language (June 2016)
66. Xu, S., Huang, Y., Pan, J., Ma, Z., Chai, J.: Inversion-free image editing with natural language. arXiv preprint arXiv:2312.04965 (2023)
67. Xu, S., Ma, Z., Huang, Y., Lee, H., Chai, J.: Cyclenet: Rethinking cycle consistent in text-guided diffusion for image manipulation. In: Advances in Neural Information Processing Systems (2023)
68. Zhang, D.J., Wu, J.Z., Liu, J.W., Zhao, R., Ran, L., Gu, Y., Gao, D., Shou, M.Z.: Show-1: Marrying pixel and latent diffusion models for text-to-video generation. arXiv preprint arXiv:2309.15818 (2023)
69. Zhang, L., Rao, A., Agrawala, M.: Adding conditional control to text-to-image diffusion models. In: Proceedings of the IEEE/CVF International Conference on Computer Vision. pp. 3836–3847 (2023)

70. Zhang, Y., Xing, Z., Zeng, Y., Fang, Y., Chen, K.: Pia: Your personalized image animator via plug-and-play modules in text-to-image models. arXiv preprint arXiv:2312.13964 (2023)